Rational Design of a Novel Highly Folding-tolerable Edgewo-rthia Chrysantha Lindi-derived Substrate for Versatile Flexible Pressure Sensors

Danning Fu
South China University of Technology
Ruibin Wang
University of South China
Rendang Yang (rendangyang@163.com)
South China University of Technology https://orcid.org/0000-0002-5928-9852

Research Article

Keywords: underutilized biomass, silver nanowires, conductive paper, flexible electronics, monitoring human motions

Posted Date: December 8th, 2021

DOI: https://doi.org/10.21203/rs.3.rs-1113986/v1

Abstract

Cellulose-based composites with superior mechanical and electrical properties are highly desirable for a sustainable and multifunctional substrate of flexible electronics. However, their practical application is hindered by the lack of superflexible cellulose-based composites to fabricate ingenious flexible electronics with considerable robustness. Here, cellulose derived from underutilized biomass (*Edgeworthia chrysantha Lindi*, ERCL) was composited with highly-conductive silver nanowires (AgNWs) through a general papermaking process. Benefiting from the interactions between cellulose and AgNWs including hydrogen bonding and van der Waals force, the composite presented superb electrical conductivity (> 27000 S/m) and flexibility (folding times ≥1110). By employing it as the substrate of flexible pressure sensors (FPSs) through layer-by-layer assembly, improved sensitivity (Gauge Factor=846.4), rapid response (0.44 s), and excellent stability (≥2000 folding cycles) were demonstrated. Impressively, the novel FPS could monitor human motions, including finger bending, elbow flexion, speaking, and pulse, suggesting its great potentials in emerging flexible electronics.

1. Introduction

In the era of internet of things (IoT), flexible electronics, which can maintain the efficiency of work under certain deformation (bending, folding, twisting, compression, and stretching) conditions, have become one of the state of art trends of technology. The applications of flexible electronics including flexible pressure sensors (FPSs), electronic skins, foldable touch screen, artificial intelligence, which further prove their versatile way into daily life (Lyu et al. 2021). The outbreak of the COVID pandemic since 2019 further accelerates the development of flexible electronics, such as the application scenarios of temperature monitoring. Compared to conventional rigid and planar materials, the materials as the substrate of flexible electronics inherently have the merits of elasticity and conformality, required to withstand extreme mechanical deformations, as well (Chen et al. 2019; Seo and Hwang 2019; Zhang et al. 2019; Nie et al. 2020; Xue et al. 2020). Most synthetic polymers, such as polyethylene terephthalate (PET) (Li et al. 2019), polydimethylsiloxane (PDMS) (Guan et al. 2020), thermoplastic polyurethane (TPU) (Zhang et al. 2020; Wu et al. 2021), polyethylene glycol (PEG) (Chen et al. 2018), polyimide (PI) (Fang et al. 2018), Ecoflex (Kim et al. 2018), poly(1,1-difluoroethylene) (PVDF) (Tai and Lubineau 2017), to name a few, have been used to fabricate flexible electronics as substrate. However, the problems include non-recyclability, high cost, immune exclusion, mechanical and thermal instability (Bhatia et al. 2021). As such, it is of great significance but still challenging to explore recyclable, low-cost, biocompatible, mechanically, and thermally stable substrates.

Cellulose, which is of renewability, low cost, easy processability, biodegradability, and attractive physical performances, has been frequently introduced into composites as the sustainable alternative of synthetic polymers to support or bind flexible electronics (Chen et al. 2021; Zhao et al. 2021). For instance, Yong et al. (Wei et al. 2016) utilized a convenient dip-coating method to transfer conductive materials to the cotton sheet. It was revealed that the obtained FPS was endowed with a sensitivity of 3.4 kPa^{-1}, a fast response speed of 50 ms, and prominent working stability (high electrical conductivity remains

unchanged after 500 load-unload cycles). A printing paper-based conductive composite was obtained via a coating, using PDMS liquid as the intermediate dielectric layer to form a self-assembled sandwich structure, which could be used to manufacture flexible capacitive sensors (Li et al. 2019). Due to its advantages of high efficiency, good uniformity and strong adhesion, the obtained cellulose-based composite showed good potential in detecting human activities. In addition, highly porous tissue papers were employed as an appealing substrate to fabricate flexible electronics by Huang et al. (Huang et al. 2020) The tissue paper was pretreated with NaOH to destroy the hydrogen bonds between cellulose molecules, thereby promoting the expansion of cellulose fibers and improving the sensitivity of this composite-based pressure sensors. However, the mechanical and sensing properties of the sensors listed above still cannot meet the needs of next-generation FPSs. Thus, it is vital to develop more robust cellulose-based materials as a flexible substrate and enhance the sensitivity at the same time.

Edgewo-rthia chrysantha Lindi (ERCL), also known as Xue hua pi, is an evergreen shrub that belongs to *Daphne odora*. The fibers of ERCL are densely distributed, lengths of 2.9~4.5 mm (The common fiber length of hardwood is 1 mm, and for softwood is 2~3 mm.). As a kind of underutilized biomass, it was once used in the papermaking industry (including leather paper, firecracker paper, and oil paper), paper-based umbrella, fan, oil basket, pasting window, and other fields (Wang and Zhang 1985), as shown in Fig. 1. Apparently, the outstanding traits of ERCL, such as flexibility, toughness, bright white, glossiness, and superb tensile strength, have not been fully exploited throughout the applications mentioned above, resulting in massive waste. Therefore, it is meaningful to broaden its application into the state of art technologies. To treat ERCL as substrate would provide numerous possibilities in the creation of soft materials for new flexible electronics. And it is of great significance to explore their multifunctional sensing behavior as FPSs (Liu et al. 2017; Pu et al. 2019; Su et al. 2019; Yin et al. 2020).

Herein, underutilized, valuable biomass was developed to fabricate a novel cellulose-based composite consisting of a highly-conductive AgNWs percolation network through a facile papermaking process by serving the ERCL fiber as the matrix. As a typical demonstration, in addition to the tensile strength, the obtained composite delivered an impressive folding endurance with folding times of 1110 arising from the entanglement of fiber and AgNWs, the appropriate length of ERCL fiber as well. Additionally, remarkable sensing performance was also observed. Thanks to the above advantages, the designed FPS based on this novel composite substrate exhibited high conductivity, improved sensitivity, rapid response, and stability. Excitingly, the multifunctional sensing behaviors, such as finger bending, elbow flexion, speaking, and pulse monitoring could also be achieved by the robust and sustainable FPS, promising its great potentials as flexible smart robots.

2. Materials And Methods

2.1. Synthesis of AgNWs

For a typical synthesis of AgNWs, a one-pot reaction was employed to mix all chemicals and solvents. Firstly, 0.2 g of polyvinylpyrrolidone (PVP) was added to 25 mL of ethylene glycol (EG) and completely

dissolved using magnetic stirring in a water bath at 60°C. After obtaining a transparent and uniform solution, cooled down to room temperature. Then, 0.25 g of silver nitrate ($AgNO_3$) was added to the PVP solution, rapid agitation was required so as to dissolve the solute completely. After that, 3.5 g of ferric chloride ($FeCl_3$) salt solution (600 μM in EG) was poured into the mixture and stirred for 1~2 minutes. The mixture was then immediately transferred into an oil bath preheated at 130°C to grow AgNWs for 5 h until the reaction finished. Lastly, acetone and ethanol were used to wash the precipitate with centrifugation of 9000 rpm for 10 min. The AgNWs were re-dispersed in ethanol (≈0.2 wt%) for further use (Jiu et al. 2014).

2.2. Fabrication of cellulose/AgNWs composite paper (CACP)

The ERCL fiber was obtained through a traditional alkaline pulping (cooked in the calcium hydroxide solution and sodium carbonate solution successively). The degree of beating 35°SR. The content of three components (including cellulose, hemicellulose, and lignin) in ERCL was 72.9%, 17.2%, and 6.8%, respectively (Sluiter et al. 2010). The papers used in the dipping method and vacuum filtration were made by rapid Kothen-method with laboratory sheets former in advance. (i) As for the dip-coating method, the D-CACP was fabricated through an impregnation process. Specifically, CACP was submerged in the AgNWs dispersion for different dipping times (from 0 to 5 times with a step size of 1 min). The coated paper was then dried in a vacuum drying oven at 60°C for 15 min. (ii) Vacuum filtration was utilized for the preparation of V-CACP. Cellulose filter membrane substrate was placed inside the Bucher funnel and AgNWs dispersion (10~40 wt%) was added into it. AgNWs were trapped within the pores of the paper substrate and ethanol was drawn through the funnel. The obtained paper was then dried in the vacuum drying oven at 60°C for 15 min. (iii) W-CACP was fabricated by wet-forming (papermaking) process. The ERCL fiber was mixed fully with AgNWs, and then the paper was made by papermaking process. The resultant W-CACP was then transferred to a roller dryer at 60°C. The total experiment procedure of this study is depicted in Fig. 2.

2.3. Fabrication of the W-CACP based FPS

The FPS was fabricated to evaluate the sensing performance of W-CACPs with different content of AgNWs. The obtained W-CACP was first cut into strips with a dimension of 30 mm × 10 mm × 0.121 mm, and the two ends of them were pasted with copper tape to fix them to the electrochemical workstation so as to verify its sensing properties. The whole sensing system was encapsulated with transparent 3M tape.

2.4. Characterization

Field emission scanning electron microscope (FE-SEM Merlin, Zeiss, Germany) was carried to explore the surface and cross-sectional morphologies of AgNWs, ERCL fiber, and CACP. The test was carried out at an accelerating voltage of 5 kV. Samples were spray-coated with gold using the auto-fine sputtering unit. The change of chemical structure of CACP before and after AgNWs loading was analyzed by Fourier Transform infrared spectroscopy (FTIR Nexus 470, Thermo Nicolet). The wavenumbers were collected in

the range of 4000~400 cm^{-1} using a Nicolet Nexus 870 spectroscopy in an attenuated total reflection (ATR) mode at room temperature. The mechanical performance was acquired by a folding tester (MIT/U21B, USA) and a material testing machine (INSTRON 3300, England). The thermal stability of the W-CACP was analyzed through a thermal gravity (TG) analyzer (STA449F3, NETZSCH, Germany) at a heating rate of 10°C/min in the range of 30~800°C under nitrogen gas ambiance. Electrical conductivity was measured by a four-probe tester (RTS-8, 4 PROBE TECH, China), digital multimeter (VICTOR VC890C, China), and electrochemical workstation (CHI 750 E, China). The sensing performance of W-CACP was tested by an electrochemical workstation and electronic universal testing machine (SHIMADZU, Japan). Herein, the sensitivity of the sensor was assessed by gauge factor (G.F), and G.F is defined below:

$$G.F = \frac{\Delta R/R0}{\varepsilon}$$

1

where the $\Delta R/R_0$ is defined as the ratio of the resistance change (ΔR) to the resistance (R_0) at the initial state; ε is the mechanical strain. At least ten specimens were tested for each sample and the results were reported as average.

3. Results And Discussion

3.1. Comparisons of D-CACP/V-CACP/W-CACP

3.1.1 Morphology

Figure 3 shows the SEM images of AgNWs, ERCL fiber, and CACP, respectively. Overall, Fig. 3a and Fig. 3f-g show the AgNWs had a length of over 14 μm, and a diameter of about 80 nm (aspect ratio of 175). The SEM images also indicate that the AgNWs were synthesized almost without any Ag nanoparticle, verifying the purity of AgNWs, which was a significant factor for the performance of AgNWs based composites. From Fig. 3b, it is clear that ERCL fibers were flat, and there were evident holes between those fibers, both of these features were conducive to the attachment of AgNWs to cellulose paper. Moreover, Fig. 3b establishes the length of pristine fibers reached more than 3 mm, and the average width was between 12 to 33 μm. Generally speaking, the mechanical characteristics, especially for the tearing strength, tensile strength, bursting strength, and folding strength of the paper, can be enhanced with the increase of fiber length. In theory, the optimal length of fiber in the papermaking industry is 1.5~5 mm. The fibers with an average length less than 0.4 mm are not appropriate to be used as raw materials to make paper, though can be treated as filler in the papermaking process. On the other hand, if the fibers are too long (especially for the average length is more than 5 mm), which will lead to the heterogeneity of acquired paper. More specifically, the pulp is apt to coagulate, resulting in “cloud flower” paper. Thus, the long-time beating process is not necessary for ERCL, whose fiber length (2.9~4.5 mm) is quite perfect in the papermaking industry. This feature is conducive to further cut down the cost of the production of

ERCL paper. In addition, the width of fiber is another vital indicator in papermaking, for it is closely related to the interweaving ability among fibers. For instance, the strength of paper made of Eucalyptus is superior to the paper made of poplar, because of the smaller average fiber width of Eucalyptus (Fu et al. 2020). It is evident that ERCL fiber behaves as a uniqueness with a more appealing length and diameter than common fiber, which will facilitate the entanglement with AgNWs.

As shown in Fig. 3c-d (D-CACP and V-CACP), AgNWs were non-uniformly deposited on the surface of the paper, only a few AgNWs were found to be embedded between the holes of the paper, which were caused by the gap among the fibers. The content of AgNWs loaded by vacuum filtration was higher than that loaded by impregnation, which demonstrated vacuum filtration process was a more efficient method than dip-coating for the fabrication of CACP. More interestingly, the connection between fiber and AgNWs (W-CACP) was much more compact as shown in Fig. 3e, which was extremely conducive to enhance the conductivity of paper.

3.1.2 Chemical structure

In order to prove there is no chemical bonding between fiber and AgNWs, the FTIR spectra of the D-CACP, V-CACP, W-CACP, and pure ERCL paper are shown in Fig. 3h. All of the samples showed a characteristic absorption band of cellulose from 3100 cm^{-1} to 3700 cm^{-1}, which indicated the strong stretching vibration of the hydroxyl group. The absorption peak at 2889 cm^{-1} is attributed to the C-H symmetric vibration peak of methylene (-CH_2-). And the peak at 1645 cm^{-1} corresponds to the bending vibration of the hydroxyl group absorbing water. The characteristic peak at 1369 cm^{-1} is due to the antisymmetric bending vibration of C-H, while the peak at 1058 cm^{-1} and 892 cm^{-1} are due to the C-O stretching and C-H rocking vibrations of cellulose (Sun et al. 2000; Xiao et al. 2001; Himmelsbach et al. 2002; Sain and Panthapulakkal 2006; Alemdar and Sain 2008; Trache et al. 2014). It is noteworthy that the absorption peak of stretching vibration of -OH moved to the lower wavenumber after the cellulose paper was loaded with AgNWs. It was probably because the hydrogen bond stretching of cellulose was strengthened by residual PVP on AgNWs, for a large number of hydrogen bonds would be formed by carbonyl on PVP molecule and hydroxyl groups in cellulose (Qian et al. 2017). That is to say, the appropriate amount of residual PVP played a positive role in the fabrication of CACP, otherwise, the conductivity of paper might be decreased in a way. Notwithstanding, it is worth mentioning that there was no direct chemical binding between AgNWs and fiber among the three methods.

3.1.3 Electrical property

Electrical property is considered to be the most critical performance of a pressure sensor. In this study, CACP was prepared through three different techniques. And the optimum electrical conductivity of CACP was influenced by the number of dipping times and the content of AgNWs. The results (Fig. 3i) established that the electrical conductivity increased sharply upon increasing the dipping times, which was probably due to more AgNWs accumulated in the intervenes of fibers with the increasing of the number of dipping times. In conclusion, the electrical property was enhanced as the dipping times

increased. However, the content of AgNWs on paper was limited, redundant AgNWs loosely settled on the surface of CACP, and they would fall down easily after drying. And from Fig. 3i, it could be concluded that four may be the optimal number of dipping times, in this study, the AgNWs content was about 10 wt%. Apparently, the content of AgNWs was restricted in a dip-coating process (the electrical conductivity almost maintained unchanged after dipping four times). Moreover, it was essential to provide a great quantity of AgNWs dispersion in the impregnation process, resulting in the waste of raw materials and increased cost.

Both the methods (vacuum filtration and wet-forming method) attained the high AgNWs content. Upon increasing the AgNWs content from 10 wt% to 30 wt%, the electrical conductivity of V-CACP almost rose to 25000 S/m (Fig. 3j), while the electrical conductivity of W-CACP reached more than 27000 S/m (Fig. 3k). In addition, the uneven distribution of AgNWs could lead to heterogeneity of the surface electrical characteristic of CACP. Compared with the vacuum filtration method, the wet-forming method might be more favorable for the production of CACP, for AgNWs and fibers were well mingled during the fabrication process. AgNWs content of about 30 wt% was considered a desirable and affordable condition for the future sensor studies.

Collectively, it can be convincingly inferred that the three methods mentioned above were potential methods to fabricate CACP, while the wet-forming process was confirmed to be the most effective way, due to the maximum content of AgNWs that accumulating on the surface of fibers and the uniformity of obtained CACP. Besides, the connection between AgNWs and fibers was the tightest as shown in the SEM images. As a consequence, the electrical conductivity performed marvelously of paper made through wet-forming process. The samples acquired by the wet-forming technique were used for further studies and analyses.

3.2. Characteristics of W-CACP

3.2.1 Mechanical performance

The digital photos, SEM images, and mechanical properties (mainly folding endurance and tensile properties) of ERCL paper as shown in Fig. 4a-e. It can be clearly seen from Fig. 4a-b that W-CACP and pure ERCL paper (W-CACP-0) possessed great reproducibility after numerous folds. And the surface of W-CACP became smoother owing to the introduction of AgNWs. Besides, the interconnection between fibers and AgNWs hardly be destroyed by bending, which proved that the stable combination between conductive matrix and building blocks. The results of optical analysis paved the way for further mechanical tests.

3.2.1.1 Folding strength/folding endurance

Figure 4c shows the folding performance of obtained W-CACP under 0 wt%, 10 wt%, 20 wt%, and 30 wt% content of AgNWs, respectively. The folding strength/folding of paper is closely related to the length, width, strength, and flexibility of fiber. Interestingly, pure ERCL paper represented the marvelous folding

strength, whose fold number (>1800) was more than 50 times that common paper (about 36) under the same weight of paper. The phenomenon might be attributed to the proper length and width of ERCL fiber. Moreover, the ratio of cell wall thickness to cell cavity diameter represents the coefficient of flexibility. The contact area among various fibers of paper increases with the decrease of the ratio of wall to the cavity, thus the bonding force is stronger so as to attain the paper with high strength. In contrast, the fibers with a larger wall to the cavity ratio are more rigid, resulting in a smaller contact area and a weaker binding force between fibers, ultimately bringing about the poor mechanical strength of paper. While 10 wt% of AgNWs was added into the composite, the folding number slightly fell, still maintained at a high level (>1500). This was possibly caused by the weakened connection between fibers because of the embedded AgNWs of W-CACP. As the content of AgNWs increased, the brittleness of W-CACP rose, too. It is important to note that the folding endurance of the W-CACP was superb in this study. Thus, it is envisioned that W-CACP has promising applications in wearable electronic devices.

3.2.1.2 Tensile properties

In addition, Fig. 4d-e reveals that the tensile properties of W-CACP (W-CACP-1, W-CACP-2, and W-CACP-3) and pure ERCL paper (W-CACP-0). It has been established that the tensile strength and Young's modulus of pure ERCL paper were 49.3 MPa and 1298.4 MPa, respectively. Correspondingly, both of the tensile strength and Young's modulus of W-CACP-3 presented an upward tendency, and the increase of about 48.7% and 34.9% was observed for them. It was probably ascribed to the introduction of AgNWs into CACP brought about the rigidity, so as to improve tensile properties of CACP. Significantly, when the AgNWs content was less than 30 wt%, the tensile strength decreased with increasing the AgNWs content. Especially for the AgNWs content at 20 wt% (W-CACP-2), the reduction of tensile strength and Young's modulus were 64.3% and 76.2%, respectively. As for Young's modulus, it started with an increase for a lower AgNWs content (10 wt% for W-CACP-1), while a decline trend for higher AgNWs content (20 wt% for W-CACP-2). Afterwards, the Young's modulus rose again when the content of AgNWs reached 30 wt%. It could be convincingly inferred that low content AgNWs were not sufficient to provide enough electrical conductivity with outstanding tensile properties, instead, affect the intrinsic connection between fibers, thus leading to the weakness of tensile properties. It probably due to the phenomenon of uneven distribution of AgNWs turned to be defects owing to the huge difference of modulus between AgNWs and fibers. Only while the content of AgNWs attains the optimum content, the modulus of the whole composite can be heightened.

3.2.2 Electrical performance

For additional analysis of electrical performance, the *I-V* characteristic curves and photographs of W-CACP connected with a LED were acquired at the same time (Fig. 4f-g). It then appeared obvious that the linear relationship between current and voltage was good, which demonstrated the outstanding stability of the conductive network. Accordingly, it meant that the output of persistent electrical signal when it was fabricated as a sensor. Particularly, while more conductive network was constructed, the resistance was diminished consequently, so that the slope of the *I-V* curve dropped sharply with the increased content of AgNWs. As for the LED test, with the increased content of AgNWs in a W-CACP, the brightness was

improved under the same voltage as well. The phenomenon further confirmed the excellent electrical performance of W-CACP.

3.2.3 Thermal performance

The TG results and corresponding differential thermal analysis (DTG) curves of W-CACP (W-CACP-1, W-CACP-2, and W-CACP-3) and pure ERCL paper as shown in Fig. 4h-i. It is obvious that there was a slight mass loss evaluated for all papers in the initial stage (<100°C), which was attributed to the volatilization of free water absorbed on the surface of fiber. With the increase of temperature, the pyrolysis temperature of the sample was accelerated. Additionally, 150℃~250℃, 250℃~390℃, 400℃~780℃ were the crystallization water (within cellulose) removal stage, oxidation and carbonization stages of cellulose, respectively. And then, it was worth pointing out that T_p (the temperature where the maximum thermal decomposition rate was observed) occurred at 368.4°C, 367.2°C, 368.8°C and 367.8°C, respectively. The temperature at complete decomposition state was about 500°C, with the residual weight were 16.39%, 19.71%, 29.31% and 35.83% for pure ERCL paper, W-CACP-1, W-CACP-2, and W-CACP-3, respectively. The phenomenon illustrated the thermal stability of W-CACP remained largely the same as specific amount of AgNWs was added to the system.

3.3. Applications of the W-CACP based FPS

3.3.1 Compression sensitivity

In this work, the application of W-CACP in the field of compression sensing was systematically studied (Fig. 4j). Specifically, the sensing performance of W-CACP was evaluated by exploring the relevance between resistance and compression strain of W-CACP. At initial compression stage, the $\Delta R/R_0$ demonstrated a significant increase as compression strain enlarged, which indicated the superb sensitivity of the obtained W-CACP based FPS. It could be explained that the porosity was reduced by the increased pressure, the contaction between insulating fibers was closer than before, thus enhancing the resistance of W-CACP. Both of W-CACP-2 and W-CACP-3 demonstrated a good linear relationship under the compression strain range from 0 wt% to 25 wt%. Furthermore, the G.F. of as-prepared W-CACP-3 attained 846.4, which meant a high sensitivity of as-prepared sensor, thus the obtained W-CACP was expected to be an appealing component for FPSs.

3.3.2 Folding/Bending sensitivity

The folding endurance is an essential indicator to determine the performance of wearable textiles. The folding/bending sensitivity of W-CACP was also evaluated by exploring the relevance between electrical conductivity and folding angle of paper. Besides, the schematic illustration of the W-CACP based FPS and *I-V* curves of the FPS under different pressure as shown in Fig. 5a-b. In this study, foldable sensing device was fabricated through connecting W-CACP with an electrochemical workstation. It can be clearly seen from Fig. 5d that the electrical conductivity increased during the folding angle changing from 180° to 15°, which proved that W-CACP had an excellent response to the folding force. In theory, when the external stress was applied to the W-CACP, the pathways of AgNWs conductive network was increased, bringing

about the enhancement of electrical conductivity, yet the excessive stress would deform the conductive network. In order to further investigate the application of the W-CACP based FPS in real-time monitoring of small deformation, the sensor was quickly folded from 30° to 90°. For each folding cycle, the W-CACP based FPS was able to respond in a short folding time. To be specific, the response current reached the largest at the position of 30°, while it immediately declined after switched to the state of 90° position. Additionally, the response current was similar under repeated folded angle, indicating that the as-fabricated FPS with high reproducibility and excellent stability.

Figure 5. The sensing properties of the obtained W-CACP based FPS. (a) Schematic illustration of the W-CACP based FPS. (b) *I-V* curves of the FPS (under different pressure). (c) *I-T* curve of the W-CACP based FPS to show the periodic response feature after finger bending (bending for 10 s after stretching for 10 s). (d) *I-T* curve of the W-CACP based FPS in response to various folding angles, insets are the digital photos of folding sensing with the W-CACP based FPS. (e) *I-T* curve of the W-CACP based FPS under rapidly repeated the motions of folding-unfolding from 30° to 90°. (f) *I-T* curve of the W-CACP based FPS under repeated bending and releasing for 2000 cycles. The W-CACP based FPS was used to monitor human activities in real time: the changing current of the sensor corresponding to minimal strain change of (g) finger bending (clenching quickly after stretching for 10 s), and (h) arm bending. (i) *I-T* of the W-CACP based FPS in terms of various sound stimuli, such as “China”, “People”, and “Republic”. (j) Relative current change of the W-CACP based FPS monitoring wrist position pulse pressure. Inset are the optical images of device attached on the wrist.

3.3.3 Human motions monitoring

The W-CACP based FPS fabricated in this study was further used to monitor human motions, which had great application potential in the field of wearable electronic devices. As shown in Fig. 5c, the FPS was attached to the finger to monitor the bending of human fingers. It can be clearly seen that the response signals sent by the FPS were fast and stable. When the finger was stretched, the current maintained unchanged. While the finger was in the state of bending, the AgNWs were more closely combined with each other due to the AgNWs conductive network in W-CACP was compressed. Furthermore, the response current remained almost the same at the highest peak value, which implied that the as-fabricated FPS with outstanding reproducibility, as well. Obviously, Fig. 5h shows more stable signals of arm bending. One cause may be the greater pressure produced by arm bending than finger bending, and the larger stressed area. Thus, the stable signals are generated spontaneously.

Subsequently, our FPS was attached to the neck of a volunteer. The device was able to recognize the various words “China”, “People”, and “Republic”, as shown in Fig. 5i, indicating the high sensitivity of the W-CACP based FPS. Monitoring a person’s pulse is distinctly important for the diagnosis of some diseases. The W-CACP based FPS was pasted to the wrists of person as a pulse detector. Fig. 5j shows the real-time pulse signals recorded by the FPS when the human body was at rest. Accordingly, the FPS performed excellently in the real-time detection of people’s health. Owing to the virtues of fast response, high sensitivity and stability of the fabricated sensing system, it has potential application in real-time monitoring in the field of artificial intelligence.

4. Conclusions

In summary, we developed a novel cellulose/AgNWs composite paper (CACP) through a facile wet-forming (papermaking) process by building highly-conductive AgNWs percolation network on the cellulose matrix. Owing to the strong interactions between cellulose and AgNWs, the composite was endowed with superior robustness and high electrical conductivity (> 27000 S/m), enabling the layer-by-layer assembled FPS to exhibit excellent sensing performance (improved sensitivity (G.F=846.4), rapid response (0.44 s) and high stability (≥2000 folding cycles)). The present strategy paves the way of designing high-performance substrate/component for flexible electronics, which would find great potential applications in soft robots, electric skins, etc.

CRediT authorship contribution statement

Danning Fu: Conceptualization, Methodology, Software, Validation, Formal analysis, Writing - Original Draft. **Ruibin Wang**: Data curation, Writing - Review & Editing, Visualization, Investigation. **Rendang Yang**: Resources, Supervision, Project administration, Funding acquisition.

Declarations

Declaration of Competing Interest

There are no conflicts of interest to declare in this paper.

Acknowledgements

Funding: This work was supported by the National Key Technology R&D Program (Project's number: 2017YFB0307900).

References

Alemdar A, Sain M (2008) Isolation and characterization of nanofibers from agricultural residues-Wheat straw and soy hulls. Bioresource Technol 99:1664-1671.

Bhatia SK, Otari SV, Jeon J, Gurav R, Choi Y, Bhatia RK, Pugazhendhi A, Kumar V, Rajesh Banu J, Yoon J, Choi K, Yang Y (2021) Biowaste-to-bioplastic (polyhydroxyalkanoates): conversion technologies, strategies, challenges, and perspective. Bioresource Technol 326:124733.

Chen H, Song Y, Cheng X, Zhang H (2019) Self-powered electronic skin based on the triboelectric generator. Nano Energy 56:252-268.

Chen J, Oh SK, Zou H, Shervin S, Wang W, Pouladi S, Zi Y, Wang ZL, Ryou J (2018) High-output lead-free flexible piezoelectric generator using single-crystalline GaN thin film. ACS Appl Mater Interfaces 10:12839-12846.

Chen Z, Yan T, Pan Z (2021). Review of flexible strain sensors based on cellulose composites for multi-faceted applications. Cellulose 28:615-645.

Fang F, Huang G, Xiao H, Li Y, Hu N, Fu S (2018) Largely enhanced electrical conductivity of layer-structured silver nanowire/polyimide composite films by polyaniline. Compos Sci Technol 156:144-150.

Fu H, Mo W, Shen X, Li B (2020) Impact of centrifugation treatment on enzymatic hydrolysis of cellulose and xylan in poplar fibers with high lignin content. Bioresource Technol 316:123866.

Guan F, Xie Y, Wu H, Meng Y, Shi Y, Gao M, Zhang Z, Chen S, Chen Y, Wang H, Pei Q (2020) Silver nanowire-bacterial cellulose composite fiber-based sensor for highly sensitive detection of pressure and proximity. ACS Nano 14:15428-15439.

Himmelsbach DS, Khalili S, Akin DE (2002) The use of FT-IR microspectroscopic mapping to study the effects of enzymatic retting of flax (*Linum usitatissimum* L) stems. J Sci Food Agr 82:685-696.

Huang Y, Wang Z, Zhou H, Guo X, Zhang Y, Wang Y, Liu P, Liu C, Ma Y, Zhang Y (2020) Highly sensitive pressure sensor based on structurally modified tissue paper for human physiological activity monitoring. J Appl Polym Sci 137:48973.

Jiu J, Araki T, Wang J, Nogi M, Sugahara T, Nagao S, Koga H, Suganuma K, Nakazawa E, Hara M, Uchida H, Shinozaki K (2014) Facile synthesis of very-long silver nanowires for transparent electrodes. J Mater Chem A 2:6326-6330.

Kim D, Yoon Y, Kauh SK, Lee J (2018) Towards sub-microscale liquid metal patterns: cascade phase change mediated pick-n-place transfer of liquid metals printed and stretched over a flexible substrate. Adv Funct Mater 28:1800380.

Li S, Huang S, Xu F, Xiao H, Zhang F, Zhang G (2019) Preparing polyester/carbon multifunctional fabrics by phosphoric acid carbonization. Cellulose 26:8907-8917.

Li W, Xiong L, Pu Y, Quan Y, Li S (2019) High-performance paper-based capacitive flexible pressure sensor and its application in human-related measurement. Nanoscale Res Lett 14.

Liu S, Li J, Shi X, Gao E, Xu Z, Tang H, Tong K, Pei Q, Liang J, Chen Y (2017) Rollerball-pen-drawing technology for extremely foldable paper-based electronics. Adv Electron Mater 3:1700098.

Lyu Q, Gong S, Yin J, Dyson JM, Cheng W (2021) Soft wearable healthcare materials and devices. Adv Health Mater 10:2100577.

Nie S, Hao N, Zhang K, Xing C, Wang S (2020) Cellulose nanofibrils-based thermally conductive composites for flexible electronics: a mini review. Cellulose 27:4173-4187.

Pu J, Zhao X, Zha X, Bai L, Ke K, Bao R, Liu Z, Yang M, Yang W (2019) Multilayer structured AgNW/WPU-MXene fiber strain sensors with ultrahigh sensitivity and a wide operating range for wearable monitoring and healthcare. J Mater Chem A 7:15913-15923.

Qian F, Lan PC, Freyman MC, Chen W, Kou T, Olson TY, Zhu C, Worsley MA, Duoss EB, Spadaccini CM, Baumann T, Han TY (2017) Ultralight conductive silver nanowire aerogels. Nano Lett 17:7171-7176.

Sain M, Panthapulakkal S (2006) Bioprocess preparation of wheat straw fibers and their characterization. Ind Crop Prod 23:1-8.

Seo Y, Hwang B (2019) Mulberry-paper-based composites for flexible electronics and energy storage devices. Cellulose 26:8867-8875.

Sluiter JB, Ruiz RO, Scarlata CJ, Sluiter AD, Templeton DW (2010) Compositional analysis of lignocellulosic feedstocks. 1. Review and description of methods. J Agr Food Chem 58:9043-9053.

Su Y, Yuan S, Cao S, Miao M, Shi L, Feng X (2019) Assembling polymeric silver nanowires for transparent conductive cellulose nanopaper. J Mater Chem C 7:14123-14129.

Sun RC, Tomkinson J, Wang YX, Xiao B (2000) Physico-chemical and structural characterization of hemicelluloses from wheat straw by alkaline peroxide extraction. Polymer 41:2647-2656.

Tai Y, Lubineau G (2017) “Self-Peel-Off” Transfer Produces Ultrathin polyvinylidene-fluoride-based flexible nanodevices. Adv Sci 4:1600370.

Trache D, Donnot A, Khimeche K, Benelmir R, Brosse N (2014) Physico-chemical properties and thermal stability of microcrystalline cellulose isolated from Alfa fibres. Carbohyd Polym 104:223-230.

Wang M, Zhang Z (1985) Advanced papermaking raw materials-Xue hua pi. Forestry science and technology of Hunan Province.

Wei Y, Chen S, Lin Y, Yuan X, Liu L (2016) Silver nanowires coated on cotton for flexible pressure sensors. J Mater Chem C 4:935-943.

Wu G, Yang Z, Zhang Z, Ji B, Hou C, Li Y, Jia W, Zhang Q, Wang H (2021) High performance stretchable fibrous supercapacitors and flexible strain sensors based on CNTs/MXene-TPU hybrid fibers. Electrochim Acta 395:139141.

Xiao B, Sun XF, Sun RC (2001) Chemical, structural, and thermal characterizations of alkali-soluble lignins and hemicelluloses, and cellulose from maize stems, rye straw, and rice straw. Polym degrad stabil 74:307-319.

Xue C, Wu Y, Guo X, Liu B, Wang H, Jia S (2020) Superhydrophobic, flame-retardant and conductive cotton fabrics via layer-by-layer assembly of carbon nanotubes for flexible sensing electronics. Cellulose

27:3455-3468.

Yin R, Yang S, Li Q, Zhang S, Liu H, Han J, Liu C, Shen C (2020) Flexible conductive Ag nanowire/cellulose nanofibril hybrid nanopaper for strain and temperature sensing applications. Sci Bull 65:899-908.

Zhang C, Tian J, Rao W, Guo B, Fan L, Xu W, Xu J (2019) Polypyrrole@metal-organic framework (UIO-66)@cotton fabric electrodes for flexible supercapacitors. Cellulose 26:3387-3399.

Zhang S, He Z, Zhou G, Jung B, Kim T, Park B, Byun J, Chou T (2020) High conductive free-written thermoplastic polyurethane composite fibers utilized as weight-strain sensors. Compos Sci Technol 189:108011.

Zhao D, Zhu Y, Cheng W, Chen W, Wu Y, Yu H (2021) Cellulose-based flexible functional materials for emerging intelligent electronics. Adv Mater 33:2000619.

Figures

Figure 1

The camera image of ERCL and its applications in traditional industries.

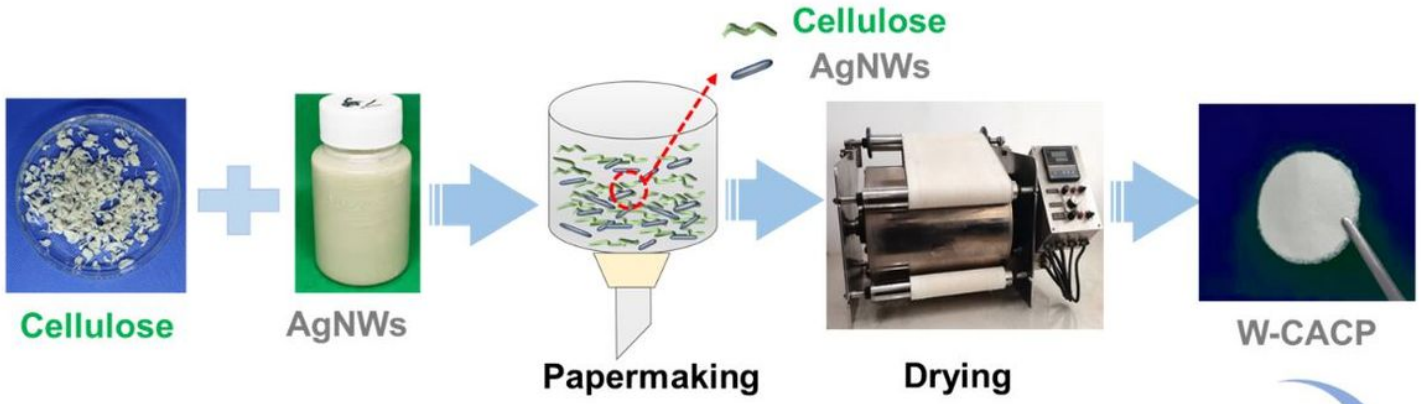

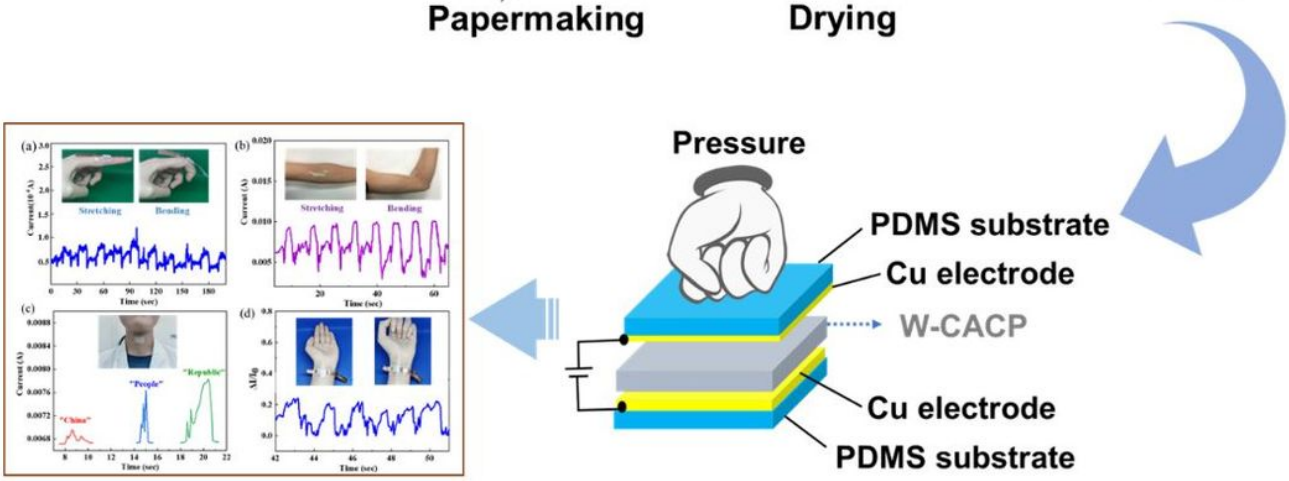

Figure 2

Schematic of fabricating the W-CACP based FPS for potential sensing application.

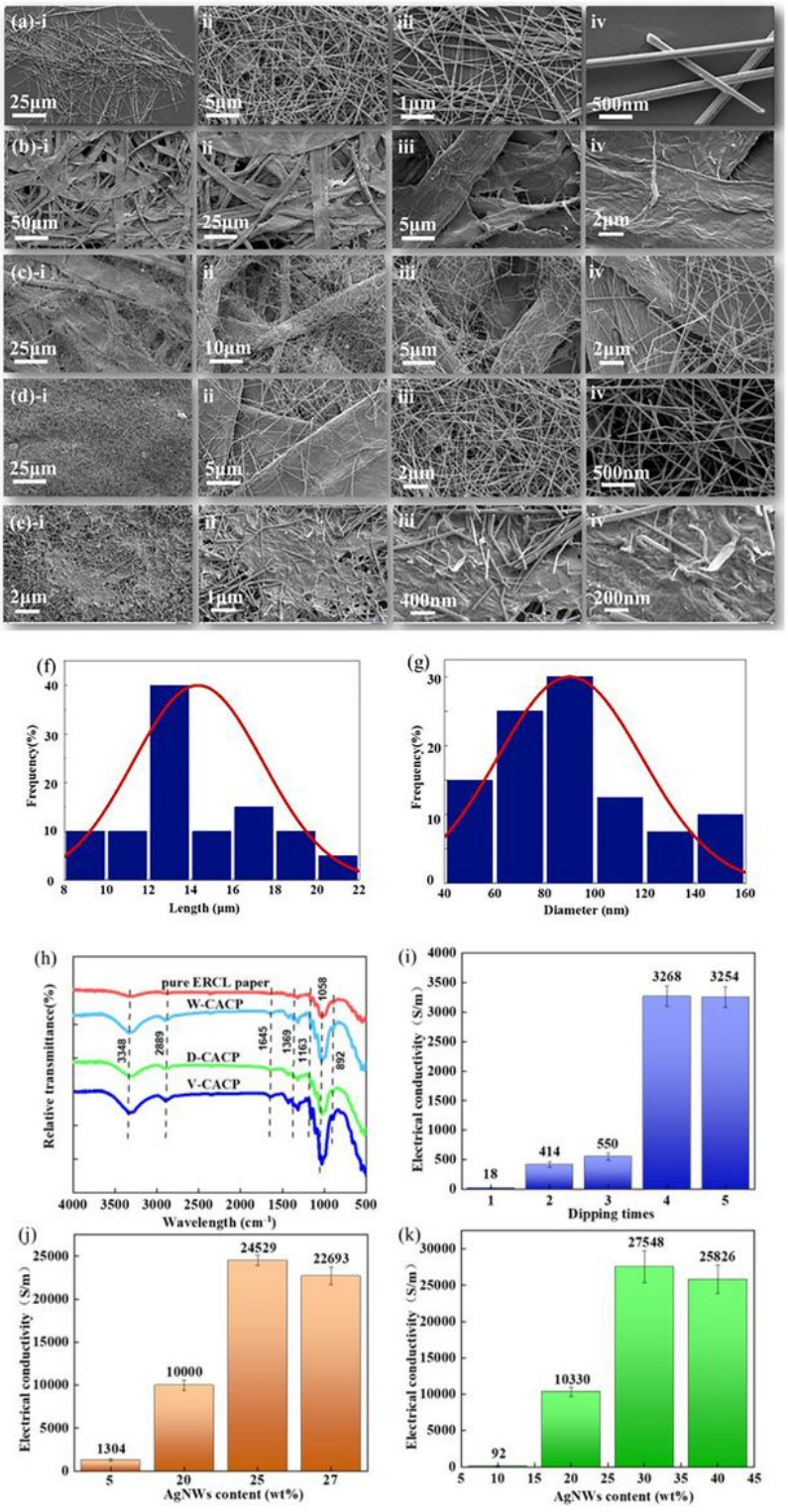

Figure 3

SEM graphs of (a) AgNWs; (b) pure ERCL paper; (c) D-CACP; (d) V-CACP; (e) W-CACP. The length (f) and diameter (g) distribution of AgNWs. (h) FTIR spectra of D-CACP, V-CACP, W-CACP and pure ERCL paper. Variation in electrical properties of (i) D-CACP with different dipping times; (j) V-CACP with different AgNWs content; (k) W-CACP with different AgNWs content.

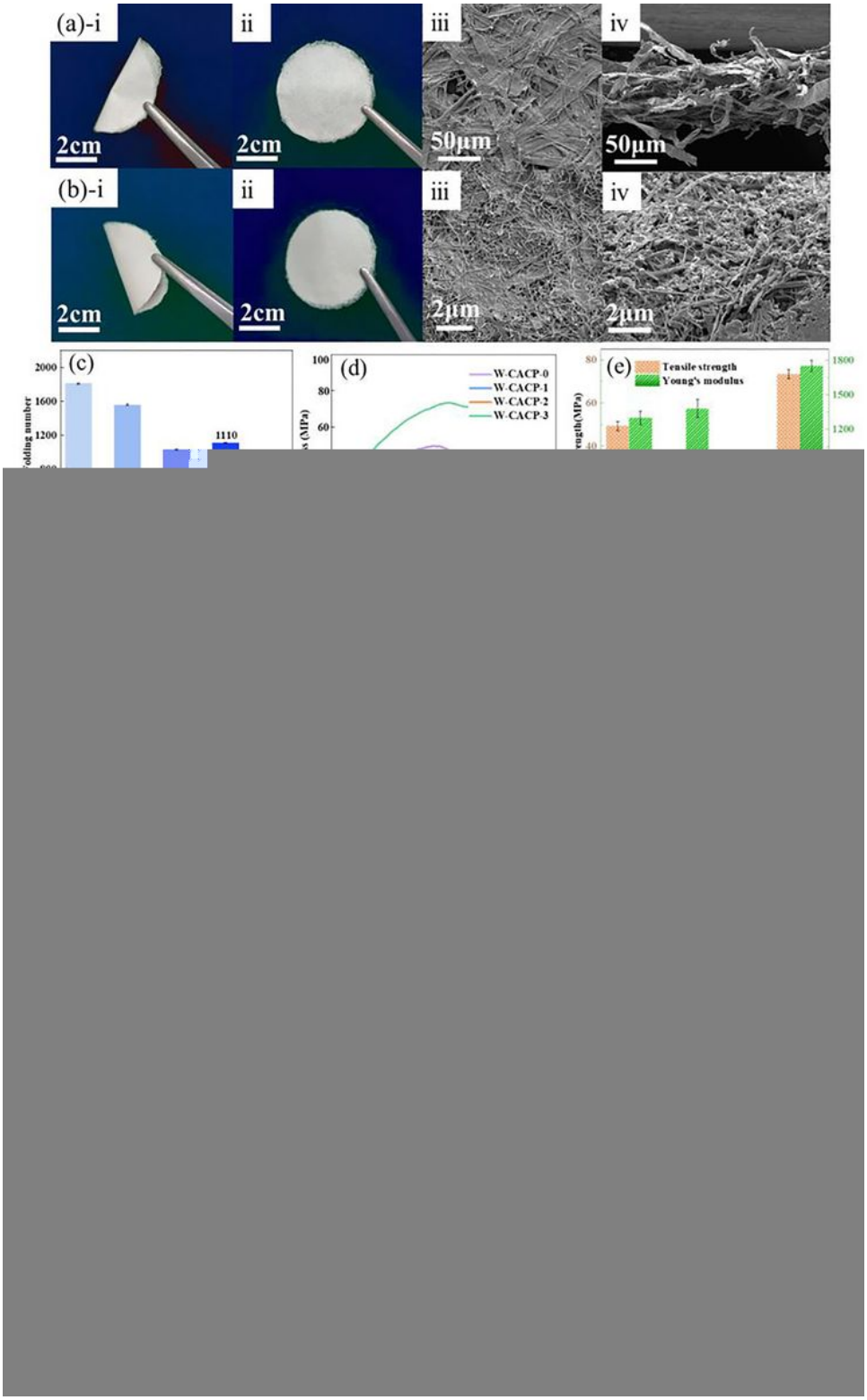

Figure 4

Digital photos of (a)-i pure ERCL paper, (a)-ii pure ERCL paper after folding cycles, (b)-i W-CACP, and (b)-ii W-CACP after folding cycles; (a)-iii and iv are SEM pictures of the surface and cross section of pure ERCL paper; (b)-iii and iv SEM graphs of the surface and cross section of W-CACP (after about 20 cycles of bending test). (c) The folding resistance of W-CACP and A4 paper; (d) The stress-strain curves of W-CACP; (e) The tensile strength and Young's modulus of W-CACP. The electrical performance of W-CACP. (f)

Current-voltage curves of obtained W-CACP; (g) the demonstration experiment of showing stable electrical conductivity in a circuit with light-emitting diode and W-CACP at room temperature. (h) TG and (i) DTG curves of W-CACP. (j) Compression test of the W-CACP based FPS.

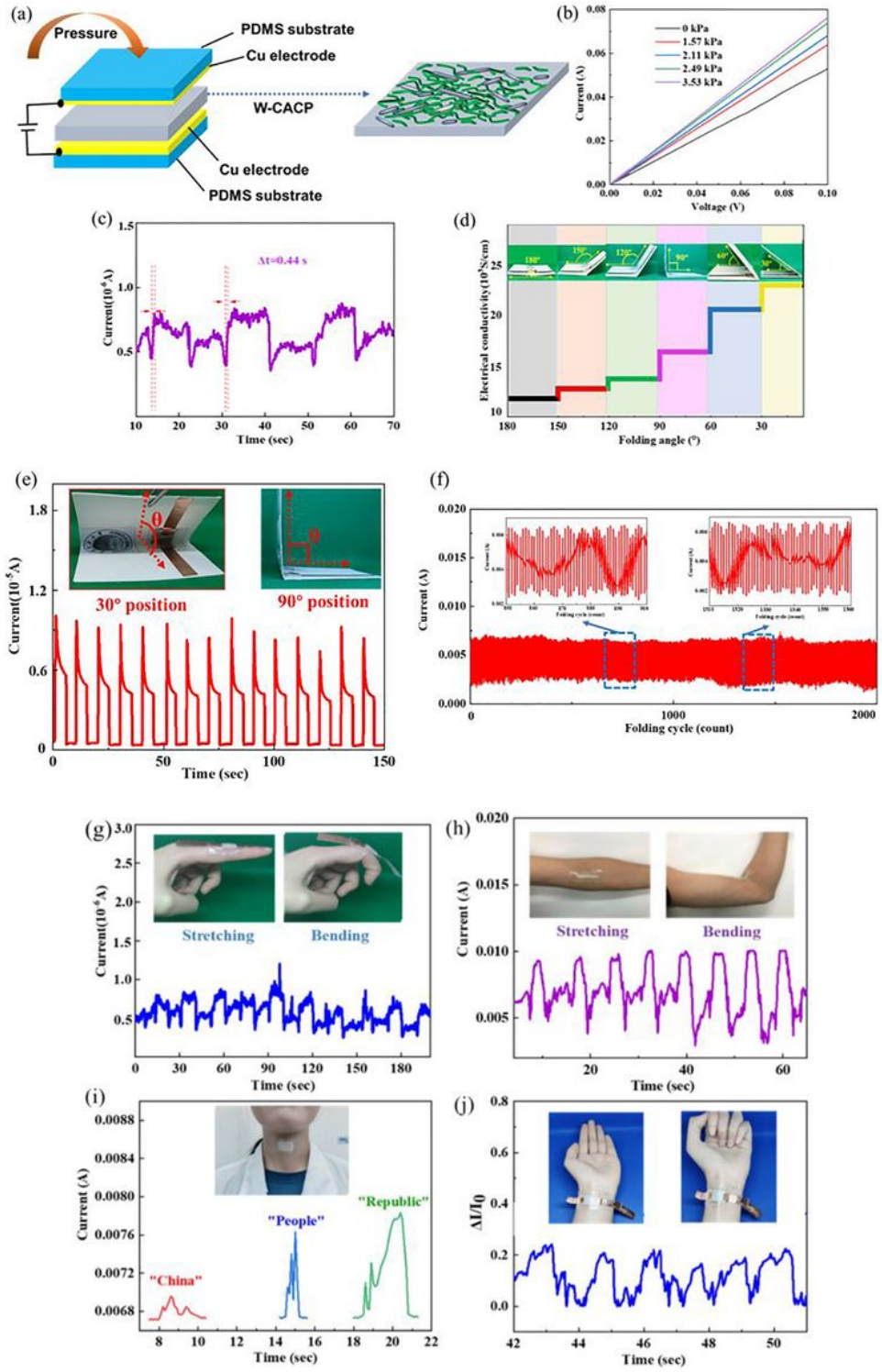

Figure 5

The sensing properties of the obtained W-CACP based FPS. (a) Schematic illustration of the W-CACP based FPS. (b) I-V curves of the FPS (under different pressure). (c) I-T curve of the W-CACP based FPS to

show the periodic response feature after finger bending (bending for 10 s after stretching for 10 s). (d) I-T curve of the W-CACP based FPS in response to various folding angles, insets are the digital photos of folding sensing with the W-CACP based FPS. (e) I-T curve of the W-CACP based FPS under rapidly repeated the motions of folding-unfolding from 30° to 90°. (f) I-T curve of the W-CACP based FPS under repeated bending and releasing for 2000 cycles. The W-CACP based FPS was used to monitor human activities in real time: the changing current of the sensor corresponding to minimal strain change of (g) finger bending (clenching quickly after stretching for 10 s), and (h) arm bending. (i) I-T of the W-CACP based FPS in terms of various sound stimuli, such as “China”, “People”, and “Republic”. (j) Relative current change of the W-CACP based FPS monitoring wrist position pulse pressure. Inset are the optical images of device attached on the wrist.

Supplementary Files

This is a list of supplementary files associated with this preprint. Click to download.

- Supportinginformation.docx